PHYSICAL REVIEW B, VOLUME 65, 035315

# Adsorption of $O_2$ on Si(111)7×7 at 300 and 30 K studied by ion photodesorption and electron photoemission

G. Comtet,*[1,2] L. Hellner,[1,2] G. Dujardin,[1,2] and K. Bobrov[2]
[1]*Laboratoire pour l'Utilisation du Rayonnement Electromagnétique (LURE) Bât. 209 D, Centre Universitaire Paris-Sud, BP 34, 91898 Orsay Cedex, France*
[2]*Laboratoire de Photophysique Moléculaire Bât 210, Université Paris-Sud, 91405 Orsay Cedex, France*

(Received 12 February 2001; revised manuscript received 31 May 2001; published 21 December 2001)

Molecular oxygen adsorption on a Si(111) 7×7 surface is investigated by ion photodesorption and valence-band photoemission from very low $O_2$ exposures up to the saturation of the adatom dangling bonds. It was found that, at 30 K, the $O_2$ molecule is adsorbed dissociatively on a silicon adatom, with one oxygen atom on top of the silicon atom and one oxygen atom inserted into the silicon backbond. This single adsorption configuration is not stable at 300 K. At 300 K, the $O_2$ molecule dissociates on a silicon adatom, with two oxygen atoms inserted into the two silicon backbonds. Double-adsorption configurations, resulting from the successive adsorption of two $O_2$ molecules on the same silicon adatom, have been identified as $SiO_4$ tetrahedral-type configurations coexisting at 300 K with double adsorption configurations having four subsurface O atoms. Finally, the diffusion of $O_2$ molecules on the surface at 30 K, and their subsequent reaction on single adsorption configurations, are proposed to explain the observed time dependence of the adsorption configuration populations.

DOI: 10.1103/PhysRevB.65.035315 PACS number(s): 68.43.−h, 68.43.Tj, 73.90.+f

## I. INTRODUCTION

Molecular oxygen adsorption on a Si(111) 7×7 surface is considered to be a prototype for studying the initial stages of oxidation reactions on semiconductor surfaces. It has been the subject of a large number of studies during the last two decades,[1–19] and it may be recognized as a critical test of the reliability of theoretical calculations and experimental observations in this field. Many contradictory models of $O_2$ adsorption on a Si(111) 7×7 surface have been proposed; however, none of them has clearly emerged so far. The main difficulty is that $O_2$ adsorption critically depends on the substrate temperature, the amount of exposure, and the time passed after the exposition. Neglecting one of these factors or several can lead to a dramatic misunderstanding of the experimental observations. Among many problems under debate, the existence of a molecular metastable state prior to dissociative adsorption has been a long-standing problem, which was reactivated by several recent theoretical and experimental papers.[19–25] Hoshino and Nishioka[22] calculated the lowest potential-energy reaction paths, and found that the $O_2$ adsorption produces a molecular precursor on a Si(111) 7×7 surface. By contrast, Lee and Kang[20] derived from density-functional theory calculations that an $O_2$ molecule spontaneously dissociates on a Si(111) 7×7 surface without any metastable molecular oxygen state, and produces an "ins-ins" configuration [see Fig. 1(c)] with two oxygen atoms inserted into two backbonds of a silicon adatom. Within this model, the double adsorption configurations resulting from the adsorption of two $O_2$ molecules on the same adatom Si site have been assigned[24] either to a tetrahedral $SiO_4$ unit, i.e., an "ad-ins×3" configuration [see Fig. 1(d)], with an oxygen atom on top of the adatom and three oxygen atoms into the three backbonds of the adatom, or to an "ins×3-tri" configuration [see Fig. 1(e)] with four subsurface oxygen atoms. Simultaneously, experimental studies of the $O_2$ adsorption on a Si(111) 7×7 surfaces were performed by Kim *et al.*[19] using the $Cs^+$ reactive scattering technique, Sakamoto *et al.*[21] using ultra-violet photoelectron spectroscopy, and by Matsui *et al.*[25] using near-edge x-ray-adsorption fine structure. While Kim *et al.*[19] concluded that molecular oxy-

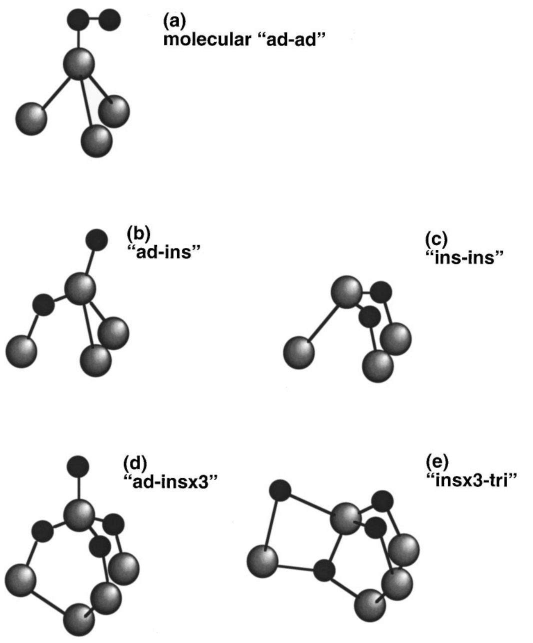

FIG. 1. Most probable adsorption configurations of $O_2$ on a Si(111) 7×7 surface. A single $O_2$ molecule has reacted with a silicon adatom site [(a), (b), and (c)]. Two $O_2$ molecules have successively reacted on the same silicon adatom site [(d) and (e)]. The large and small circles represent Si and O atoms, respectively. The drawings of adsorption configurations (b), (c), (d), and (e) were reproduced from calculated ones (Ref. 24).

gen precursors either do not exist or have extremely short lifetimes (<1 sec), Sakamoto *et al.*[21] and Matsui *et al.*[25] concluded that long-lived metastable molecular precursors do exist as molecular $O_2$ species adsorbed on top of Si adatoms stabilized by coadsorbed atomic oxygen into the backbonds.

Stimulated by these recent theoretical and experimental studies, we have performed ion photodesorption and electron photoemission experiments at 300 and 30 K in order to understand the initial stage of the $O_2$ adsorption on a Si(111) 7×7 surface. As compared to our previous investigations,[9,13,14,16] we paid special attention to the variation of the ion desorption yield and the various photoemission band intensities as a function of the oxygen exposure. From this, we have deduced that single adsorption configurations are very different at 300 K [ins-ins configuration; see Fig. 1(c)] and 30 K [ad-ins or ad-ad molecular configuration; see Figs. 1(b) and 1(a)]. Furthermore, we could identify the structure of the double adsorption configurations giving rise to photodesorption as being identical to the tetrahedral structure of silicon oxide, i.e., a silicon atom surrounded by four oxygen atoms (the so-called ad-ins×3 configuration). These assignments are accompanied with a reinterpretation of the photoemission spectra where the various bands are associated to specific chemical bonds rather than to specific adsorption configurations. Finally, we have identified a phenomenon explaining the time dependence of the $O_2$ adsorption configuration occupancy at 30 K. It consists of diffusion across the surfaces of $O_2$ molecules able to react at single adsorption configurations for producing double adsorption configurations.

## II. EXPERIMENT

The ion photodesorption and electron photoemission measurements was performed at the Synchrotron Radiation facility, SuperACO, in Orsay. The synchrotron radiation is dispersed by a grazing-incidence monochromator, which provides a linearly polarized photon source of variable energy in the 30–150-eV range. For ion photodesorption studies, the incidence angle of the photon beam (energy resolution 1 eV) on the silicon substrate is 45°, and the photodesorbed ions are collected along the direction normal to the sample by a quadrupole mass spectrometer. For UV photoemission studies, the photon beam (energy resolution 100 meV) collides with the surface at grazing incidence on the silicon substrate, and photoelectrons emitted perpendicular to the photon beam are detected. The same geometrical configuration has been chosen at 300 and 30 K, a photon incidence angle of 63.5°, and an electron detection angle of 26.5°. The overall energy resolution of the electron analysis is about 100 meV. Some O1*s* photoemission measurements have also been performed on a high-energy photon beam line of superACO. The silicon sample is cut from a silicon wafer 0.01 in. thick with a (111) orientation. The wafers are *n*-type phosphorous doped with a 1 Ω cm resistivity. The silicon sample, 25 mm long and 6 mm wide, is mounted onto a specially designed sample holder, and can be cooled down at 30 K in the analysis chamber after transfer from a preparation chamber. The temperature is measured on the molybdenum stick to which the silicon sample is attached. The silicon sample is first outgased during at least 12 h by resistive heating at 700 °C. The pressure during the last 3 h of the outgazing has to be less than $2\times10^{-10}$ mbar. Then, in order to get ride of the oxide layer, the sample is heated at 1100 °C for 30 s. During this flash, the pressure has to be less than $1\times10^{-9}$ mbar; otherwise the flash is repeated and shortened if necessary. The quality of the surface reconstruction is checked through the observation of the surface states in the electron UV photoemission spectrum. The base pressure in the UHV(ultrahigh-vacuum) chamber during the experiment is less than $4\times10^{-11}$ mbar.

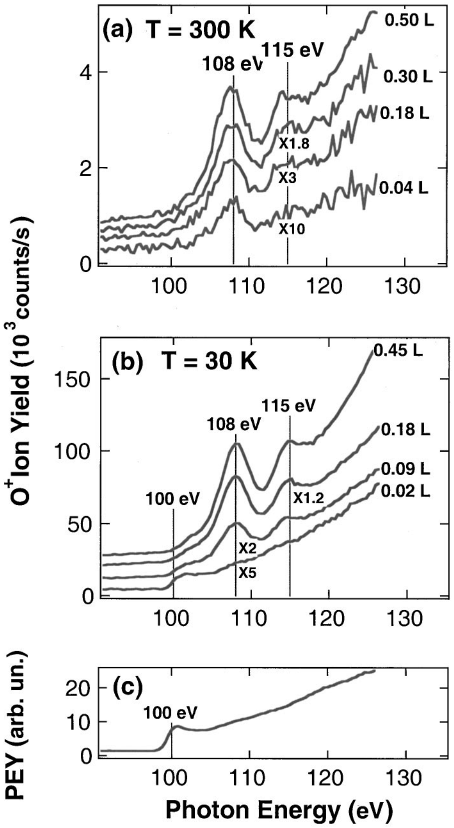

FIG. 2. $O^+$ ion desorption yields recorded as a function of the photon energy (a) for $O_2$ exposures of 0.04, 0.18, 0.30, and 0.50 L on a Si(111) 7×7 surface at 300 K, and (b) for $O_2$ exposures of 0.02, 0.09, 0.18, and 0.45 L on the Si(111) 7×7 surface at 30 K. All the $O^+$ yield curves have been normalized to the same photon flux. (c) is the electron yield curve in the same photon energy range and with the same photon energy resolution (1 eV).

## III. ION PHOTODESORPTION EXPERIMENTS

After adsorption of $O_2$ on a clean Si(111) 7×7 surface either at 300 or 30 K, the photon excitation around the Si 2*p* excitation threshold gives rise to the desorption of $O^+$ ions only (no $O_2^+$ ions are detected). The $O^+$ desorption yield has been recorded as a function of the photon energy in the 90–130 eV range for various $O_2$ exposures ranging from 0.04 to 0.5 L [1 L(Langmuir)$=10^{-6}$ Torr sec)] at 300 K [Fig. 2(a)] and from 0.02 to 0.5 L at 30 K [Fig. 2(b)]. The electron

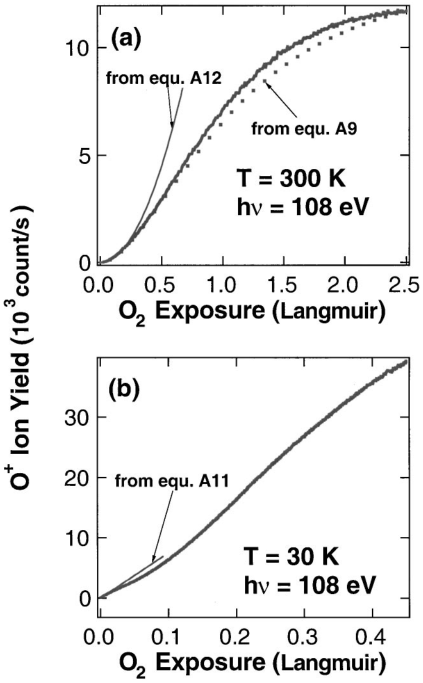

FIG. 3. $O^+$ ion desorption yields recorded as a function of the $O_2$ exposure on a Si(111) 7×7 surface at 300 K (a) and at 30 K (b), and normalized to the same photon flux. The photon energy is 108 eV. Thin curves represent the $O^+$ yields calculated from Eq. (A12) (a) and Eq. (A11) (b). The dotted curve on the upper part is the $O^+$ yield calculated from Eq. (A9) in the 0–2.5 L exposure range.

yield curve has also been recorded for comparison [Fig. 2(c)]. At 300 K, the $O^+$ desorption yield curve has always the same shape whatever the exposure [Fig. 2(a)]. On the contrary, when $O_2$ is adsorbed on the silicon surface at 30 K, the $O^+$ desorption yield curve depends markedly on the exposure [Fig. 2(b)] in agreement with Ref. 16. At very low $O_2$ exposure (0.02 L), the ion yield is similar to the electron yield curve with a step at 100 eV followed by a slight increase at higher photon energies. This step edge energy, equal to the bulk Si $2p$ excitation threshold energy, indicates that the photons are mainly adsorbed by bulk silicon atoms followed by secondary electron-induced desorption. Upon increasing the $O_2$ exposure, resonances at 108 and 115 eV appear, and then increase in intensity. Up to 0.09 L, the ion yield curve clearly shows a stepwise behavior at 100 eV. One may note that the intensity of the 108 eV resonance increases faster with exposure than that of the step function. For $O_2$ exposures higher than 0.09 L, it is difficult to distinguish the step function at 100 eV.

To find out whether the oxygen species giving rise to the observed $O^+$ photodesorption originates from the adsorption of one or two molecules on the same initial site, the exposure dependence of the $O^+$ yield has been recorded at a constant photon excitation energy of 108 eV. At 300 K, the $O^+$ desorption yield first increases quadratically and then saturates at 2.4 L [Fig. 3(a)]. The exposure dependence indicates (see Appendix A) that the $O^+$ yield originates from double adsorption configurations (two molecules have successively reacted on the same silicon site), and that the number of available initial silicon sites is limited. At 30 K, the exposure dependence of the $O^+$ desorption yield is more complicated. It first increases linearly up to 0.02 L, which indicates (see Appendix A) that the $O^+$ yield arises from single adsorption configurations. Then the yield is observed to increase less rapidly up to 0.09 L, and then more rapidly up to 0.4 L [Fig. 3(b)]. This behavior may not be associated with single or double adsorption configurations, but rather with a mixture of single or double adsorption configurations having different photodesorption cross-sections.

It is highly probable that the $O^+$ photodesorbed ions do not arise from oxygen species doubly bonded in the backbonds, but rather from singly bonded oxygen species in ad positions, i.e., on top of Si adatoms. The first reason is that it is energetically more difficult to break two bonds simultaneously than one bond. The second reason is that relaxation processes of electronically excited states are expected to be more efficient for oxygen atoms in backbonds than for oxygen in "ad" positions, since in the former case the electronic overlap, i.e., the electronic coupling with the surface should be much larger. Finally, ion desorption has been observed to occur preferentially along the normal of the sample with an angular distribution having a width of about 10°. This is also consistent with $O^+$ ions being issued from oxygen atoms in the "ad" position. However, this peaked orientation of the $O^+$ ion desorption along the normal is expected to reflect not only the direction of the Si-O bond, but also the fact that the dynamics of the ion desorption generally favours the desorption along the normal of the surface. Indeed, interaction of the desorbing ion with its image charge makes normal desorption more effective. Consequently, the $O_2$ adsorption configurations giving rise to $O^+$ desorption are considered to have at least one single-bonded oxygen atom in ad position. It follows that at 300 K, there should exist some double-adsorption configuration having at least one single-bonded oxygen atom in "ad" position, while at 30 K there should exist both single and double adsorption configurations having at least one single-bonded oxygen atom into "ad" position, their relative population depending on the $O_2$ exposure.

To characterize the double adsorption configurations giving rise to $O^+$ ion desorption, we have recorded the partial electron yield (PEY) of silicon oxide in the 90–130-eV photon energy range. Silicon samples are, prior any treatment, covered with silicon oxide. To record the PEY of this silicon oxide layer, we first carefully outgazed a silicon sample at 700 °C for 12 h. Then the surface-sensitive PEY (electrons of 35 eV kinetic energy) has been recorded in the 90–130 eV photon energy range (curve *a* in Fig. 4). This PEY is the superposition of signals from the silicon oxide layer and from the bulk Si(111). After the silicon oxide layer has been removed from the sample by heating at 1100 °C, the PEY was recorded in the same photon energy range (curve *b* in Fig. 4) and then subtracted from the surface-sensitive PEY of the silicon sample in order to get the PEY of the silicon oxide layer (curve *c* in Fig. 4). Resonances at 108 and 115 eV are in agreement with the results of Refs. 26 and 27. Theoretical calculations[28] have assigned these resonances to transitions from Si $2p$ core levels to the $t_2(3p)$ and $e(\varepsilon d)$ unoccupied molecular orbitals of $SiO_4^-$ clusters in silicon ox-

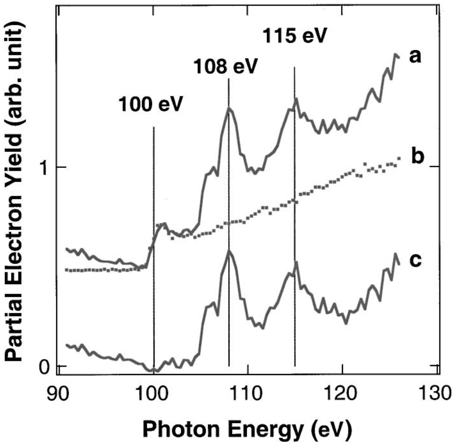

FIG. 4. Partial electron yields (35 eV kinetic energy) recorded as a function of the photon energy for the silicon sample with its oxide layer (curve *a*) and the clean silicon sample (curve *b*). Curve *b* has been adjusted in intensity to coincide with curve *a* in the 98–100-eV range. Curve *c* is obtained by subtracting curve *b* from curve *a*. The overall energy resolution is 100 meV.

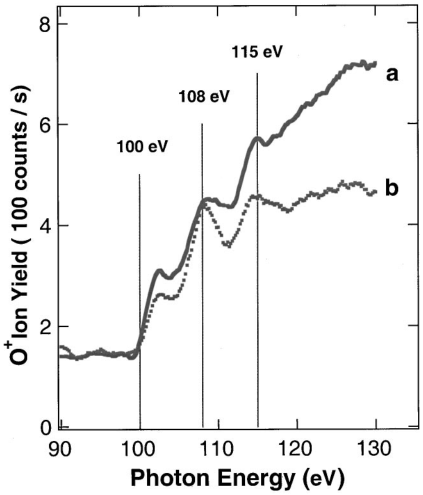

FIG. 5. Time dependence of the $O^+$ ion desorption yield curve from an $O_2$-exposed Si(111) 7×7 surface in the 90–130 eV photon energy range. Curve *a* is the $O^+$ yield curve just after an $O_2$ exposure of 0.1 L, and curve *b* is the same 20 min later.

ide. The occurrence of resonances in the $O^+$ desorption yield curve of $O_2$ on a Si(111) 7×7 surface at the same 108 and 115-eV energies suggests that the double-adsorption configurations giving rise to $O^+$ photodesorption have an atomic arrangement similar to the oxygen tetrahedral arrangement in silicon oxide. However, the precise atomic arrangement cannot be ascertained only from these resonance energies. As previously mentioned, the double-adsorption configurations, involving four O atoms and leading to $O^+$ photodesorption, have at least one single-bonded oxygen atom in an ''ad'' position. No photodesorbed $O_2^+$ ion is detected. We conclude that it is highly probable that they have an ''ad-ins×3'' configuration [see Fig. 1(d)].

We have further tested the thermal stability of the ''ad-ins×3'' configuration. After recording the $O^+$ photodesorption yield curve of Fig. 2(a) (0.48 L), we heated the sample at 250 °C for 15 sec. No $O^+$ photodesorbed ion could be detected after this thermal annealing, although the O 1*s* photoelectron spectrum is found to be unchanged. This indicates that the ad-ins×3 configuration has evolved into a configuration with the same number of oxygen atoms, all of them in subsurface position in agreement with the calculations of Lee and Kang.[24] Lee and Kang[24] called this configuration ins×3-tri [see Fig. 1(e)].

Finally, we have recorded the time dependence of the photodesorption yield curves after $O_2$ exposures of 0.04, 0.1, and 0.2 L at 30 K. The experiment has been performed as follows. After each $O_2$ exposure, a first $O^+$ photodesorption yield curve has been recorded (curve *a* in Fig. 5), the pressure in the UHV chamber being as low as $3\times10^{-11}$ mbar. Then a second yield curve has been recorded 20 min later (curve *b* in Fig. 5). The second ion yield (curve *b*) is different from the first one (curve *a*): the intensity of the previously discussed step function at 100 eV has decreased, whereas the intensity of the resonance at 108 eV has increased. The observed difference between the first and second ion yield curves cannot be due to adsorption of oxygen from the residual gas in the UHV chamber. In the considered exposure range, this would have increased both the step function feature at 100 and 108 eV resonance intensities. It cannot be due to adsorption of water from the residual gas, which would have decreased the overall $O^+$ yield curve. In a separate series of experiments, we have checked that exposures of water as low as 0.01 L quench half of the $O^+$ photodesorbed yield. The observed difference between the first and second recorded ion yields can be understood only by assuming that weakly bound $O_2$ molecules diffuse across the surface and react at single adsorption configurations to produce double adsorption configurations. This enables us to explain the decrease of the 100 eV step function intensity (single-adsorption configuration) and the increase of the 108 eV resonance intensity (double-adsorption configuration).

## IV. ELECTRON PHOTOEMISSION EXPERIMENTS

Valence-band photoemission spectra have been recorded at a photon energy of 37 eV for the clean surface and after various oxygen exposures ranging from 0.06 to 2.6 L at 300 K [Fig. 6(a)] and from 0.02 to 0.4 L at 30 K [Fig. 6(b)]. These different exposure ranges have been chosen since the saturation of the silicon adatoms occurs at an exposure of 2.4 L at 300 K and 0.45 L at 30 K. In the electron photoemission spectrum of a clean Si(111) 7×7 surface, the $S_1$ and $S_2$ bands [Figs. 6(a) and 6(b)] are associated with the dangling bonds of the silicon adatoms and restatoms of the surface respectively.[29] Upon exposure to oxygen, the intensity of the $S_1$ band decreases, the intensity of the $S_2$ band is unchanged. This means that, as previously observed,[4] the oxygen molecules interact preferentially with the adatoms. Correlatively, features appear at 1.5, 2.5, 3.8, 5.1, 7.0, 10, and 13 eV, clearly evidenced after subtracting from each photoemission spectrum the photoemission spectrum of the clean surface associated with the same photon flux. From the difference photoemission spectra normalized to the same photon flux,

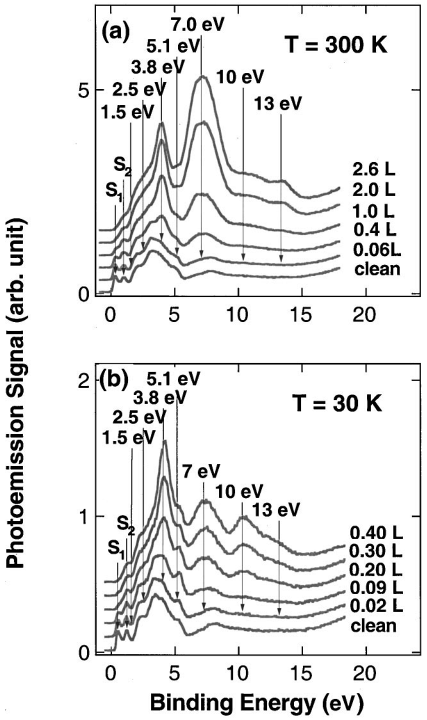

FIG. 6. Electron photoemission spectra of the clean and $O_2$-exposed Si(111) 7×7 surface. $O_2$ exposures are 0.06, 0.4, 1.0, 2.0, and 2.6 L at 300 K (a) and 0.02, 0.09, 0.21, 0.30, and 0.38 L at 30 K (b). For clarity, the photoemission spectra of $O_2$ exposed surface have been successively shifted up. All the intensities are normalized to the same photon flux. The photon energy is 37 eV (the resolution is 100 meV).

we derived the exposure dependence of the intensities of all these bands at 300 and 30 K (Fig. 7). A rigorous quantitative analysis would require a careful deconvolution of each photoemission spectrum into various surface and bulk bands. However, valuable qualitative information can be derived by simply plotting the intensity of the difference photoemission signal at certain energies as a function of the oxygen exposure.

The first comment on the data presented in Fig. 7 is that the relative intensities of the bands strongly depend on the temperature and for each temperature, on the $O_2$ exposure. One striking result concerns the relative intensities of the 3.8 and 7 eV bands. At 30 K, the 3.8 eV band intensity is always higher than the 7 eV band intensity. Conversely, at 300 K, the intensities of the 3.8 and 7 eV bands are about the same up to an exposure of 1.2 L. Then the 7 eV band continues to increase while the 3.8 eV band saturates. Lee and Kang[23] assigned low-binding-energy bands (0–4 eV) to $2p$ orbitals of oxygen atoms in ad positions and high-binding-energy bands (3.5–10 eV) to $2p$ orbitals of oxygen atoms in ins position. Consequently, we infer a stronger penetration of the oxygen atoms into the Si adatom backbonds at 300 K. Another important result concerns the intensity of the 5.1 eV band compared to those of the 3.8 and 7 eV bands. At 300 K, the intensity of the 5.1 eV band, which can be followed only up to exposures of 1.2 L due to its overlap with the 7 eV band, is always lower than those of the 3.8 and 7 eV bands.

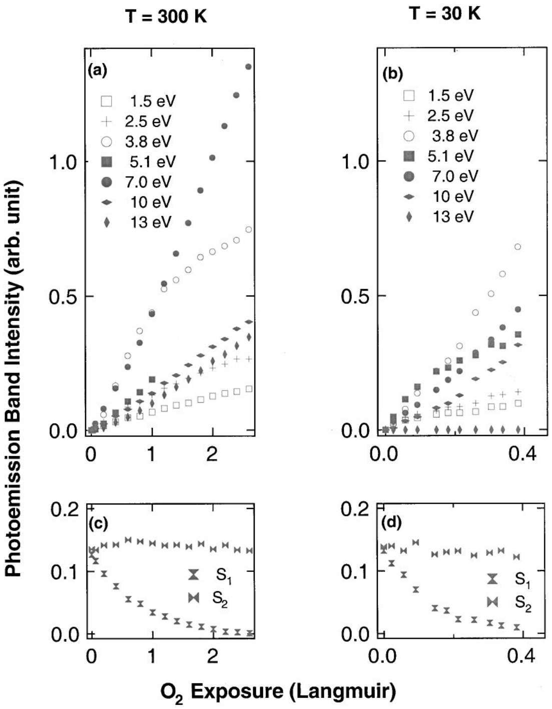

FIG. 7. $O_2$ exposure dependencies of the intensities of seven oxygen-induced bands [(a) and (b)] and of the $S_1$ and $S_2$ bands [(c) and (d)] in the electron photoemission spectra of $O_2$ on Si(111) 7 ×7 surface at 300 K [(a) and (c)] and 30 K [(b) and (d)]. All the intensities have been normalized to the same photon flux.

On the contrary, at 30 K, the intensity of the 5.1 eV band is higher than that of the 3.8 eV band up to 0.14 L, and higher than that of the 7 eV band up to 0.26 L. Both at 300 and 30 K, the intensity of the $S_2$ band remains unchanged up to the saturation of the silicon adatoms dangling bonds.

To obtain more precise information about the $O_2$ exposure dependence of the $S_1$, $S_2$, 3.8 eV, and 5.1 eV band intensities at 300 and 30 K, each of them has been recorded continuously as a function of the oxygen exposure at 300 K (Fig. 8) and 30 K (Fig. 9). The kinetic energy of the spectrometer was set at the value corresponding to one of the bands. Then the sample was flashed and irradiated after its temperature recovered. The photoemission signal was recorded for some time, without any oxygen addition, in order to obtain the base line in case of 3.8 or 5.1 eV bands. Then oxygen was rapidly introduced under a pressure of $2\times10^{-9}$ mbar, and this pressure was maintained during the recording. Let us first consider the behavior of the bands in the low-exposure regime for coverages lower than 0.2 ML [Figs. 8(a) and 9(a)]. It appears that (i) the intensity of the $S_1$ band decreases linearly, (ii) the intensity of the 3.8 eV band increases quadratically at 300 K and linearly at 30 K and (iii) the intensity of the 5.1 eV band increases linearly at both 300 and 30 K. At higher exposures [Figs. 8(b) and 9(b)], the $S_1$ band decreases exponentially both at 300 and 30 K with constants of 1.1 and 5.5 $L^{-1}$ respectively. The $S_1$ band is fully quenched at a 2.4 L exposure at 300 K and at a 0.45 L exposure at 30 K. When the $S_1$ band is fully quenched, at 300 K, the 3.8 eV

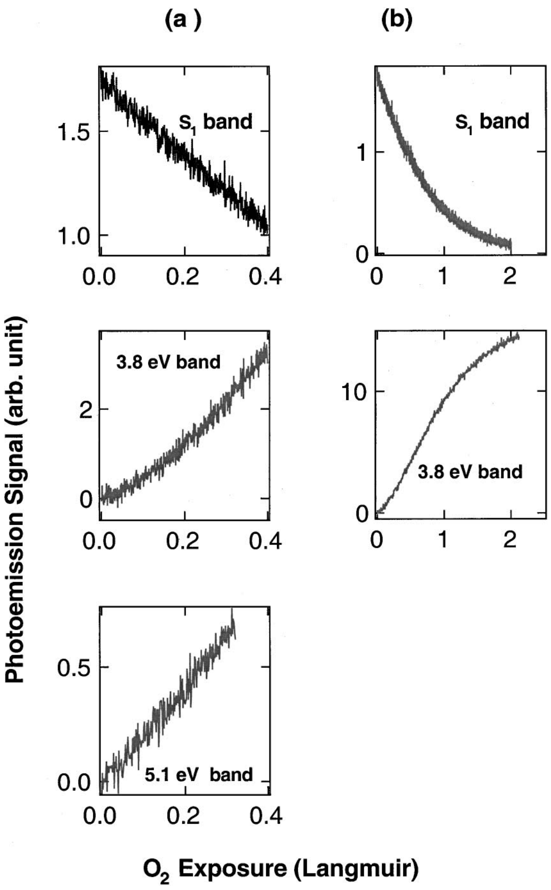

FIG. 8. $O_2$ exposure dependencies of the intensities of the $S_1$, 3.8 and 5.1 eV bands, in the electron photoemission spectrum of $O_2$ on a Si(111) 7×7 surface at 300 K. The exposure ranges are 0–0.4 L (a) and 0–2.5 L (b).

band saturates, and at 30 K the 3.8 eV band is still increasing while the 5.1 eV band saturates. Both at 300 and 30 K, the 7eV band still increases after the saturation of the silicon adatoms.

These results point out (see Appendix A) evidence of both single- and double-adsorption configurations with different relative populations at 300 and 30 K. The 3.8 eV band is associated (i) with single adsorption at 30 K and low exposures, and (ii) with double adsorption at 300 K. Conversely, the 5.1 eV band is associated with single adsorption both at 30 and 300 K. It is worthwhile to note that the same band, the 3.8 eV band for example, can be associated either with single adsorption or double adsorption, depending on the $O_2$ coverage and the temperature.

The thermal stability of the various photoemission bands after heating the sample at 250 °C for 15 sec has been tested. The 3.8 and 5.1 eV bands are quenched exactly in the same manner as the $O^+$ ion yield (see Sec. III), while the $S_1$ band associated with the silicon adatoms is unchanged and the 7 eV band intensity increases. As previously mentioned, the unchanged O 1*s* photoemission spectrum indicates that oxygen does not desorb from the surface while the 3.8 and 5.1 eV electron photoemission bands and the $O^+$ ion yield are quenched.

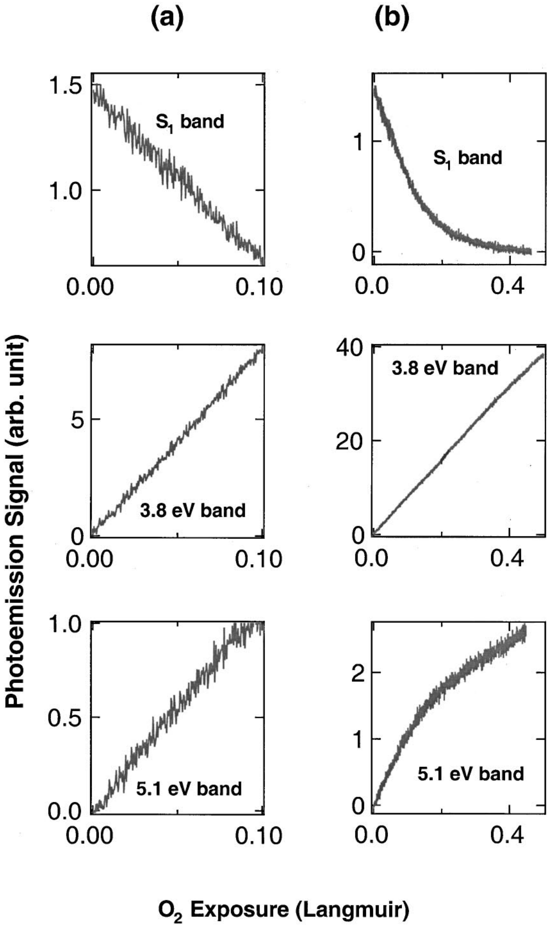

FIG. 9. $O_2$ exposure dependencies of the intensities of the $S_1$, 3.8 and 5.1 eV bands, in the electron photoemission spectrum of $O_2$ on a Si(111) 7×7 surface at 30 K. The exposure ranges is 0–0.1 L (a) and 0–0.45 L (b).

## V. DISCUSSION

The combination of ion photodesorption and electron photoemission experiments provides very useful information for understanding the adsorption of $O_2$ on a Si(111) 7×7 surface, and to assign the photoemission bands more precisely. Here we recall that ion photodesorption is considered to probe only adsorption configurations having at least one single-bonded oxygen atom in the ad position, while electron photoemission is sensitive to all adsorption configurations. Furthermore, for both ion photodesorption and electron photoemission, the observed features may be assigned either to single- or double-adsorption configurations depending on the variation of their intensities (either linear or quadratic functions) with the $O_2$ exposure.

Let us concentrate on the very low-exposure regime, associated with an oxygen coverage lower than 0.2 ML. At 30 K, ion photodesorption reveals the existence of single-adsorption configurations, with O atoms singly-bonded in ad positions [Fig. 3(b)]. It is not possible at this point to derive whether they are dissociative ad-ins and/or molecular ad-ad configurations (see Fig. 1). The three most intense oxygen-induced bands at this very low-exposure regime are the 5.1, 3.8, and the 7 eV bands. The intensities of two of them, the

3.8 and 5.1 eV bands, increase linearly with the $O_2$ exposure. According to Ref. 8, the 3.8 and 5.1 eV bands may be assigned to molecular oxygen in ‘‘ad-ad’’ configurations (see Fig. 1). Conversely, Lee and Kang’s[23] calculations suggested that (i) the 3.8 eV band corresponds to an oxygen atom in the ad position, (ii) the 5.1 eV band is correlated with an oxygen atom inserted in a Si backbond, and (iii) the 7 eV band is also correlated with an oxygen atom in a Si backbond. At 300 K, even at very low exposures, no $O^+$ ion photodesorption is observed from single-adsorption configurations [see Figs. 2(a) and 3(a)]. It follows that the single-adsorption configuration, revealed in UV photoemission by the linear dependence of the 5.1 eV band intensity as a function of the oxygen coverage, is an ins-ins configuration. This result corroborates the assignment of the 5.1 eV band to the ins oxygen atom we just suggested. In conclusion, the single-adsorption configuration observed in the low-exposure regime is not the same at 30 and 300 K. At 30 K, it may be a molecular ‘‘ad-ad’’ configuration (according to the calculations of Refs. 8 and 22) or an ‘‘ad-ins’’ configuration (according to Lee and Kang’s[20] calculations), while at 300 K it is an ins-ins configuration. This indicates that the molecular or ‘‘ad-ins’’ configuration is metastable at 30 K, in partial agreement with the calculated energy diagram for $O_2$ adsorption on a Si(111) 7×7 surface of both Refs. 8 and 22, and in complete agreement with that of Lee and Kang.[20] Indeed, the authors of Ref. 8 found an ‘‘ins-ad’’ configuration 5 eV more stable than the molecular one, but more stable than the ins-ins configuration. Hoshino and Nishioka[22] calculated a dissociative adsorption into an ‘‘ad-ins’’ configuration 3 eV lower than the metastable molecular adsorption, and did not perform calculation on the ‘‘ins-ins’’ configuration. For Lee and Kang,[20] the only metastable single-adsorption configuration is the ad-ins configuration, which may evolve into an ins-ins configuration more stable by 1.3 eV, the energy barrier between the two configurations being about 0.15 eV.

We now wish to discuss whether we can distinguish a metastable molecular ad-ad configuration from a metastable dissociative ‘‘ad-ins’’ configuration. The main argument in favor of the ‘‘ad-ins’’ structure is the observation of the 7 eV band, associated with an inserted O atom. Indeed, Lee and Kang[20] calculated the partial density of states of inserted O atoms from ‘‘ad-ins’’ configurations (with $p_z$ values) to be around 5 eV (they indicated an error of 2 eV in their calculation). Therefore, we consider that, at 30 K, the single-adsorption configurations are most probably of the ad-ins type. These configurations are metastable, and are transformed into more stable ins-ins configurations at 300 K.

At 300 K, ion photodesorption experiments revealed double-adsorption configurations having an ad-ins×3 configuration with an atomic arrangement similar to the one in silicon oxide. The exposure dependence of the 3.8 eV band intensity in the electron photoemission spectrum can be exactly superimposed to that of the $O^+$ ion yield curve at 108 eV, so that we can infer that the 3.8 eV band at 300 K is associated with the ad-ins×3 configuration. According to the calculations of Lee and Kang,[23] we assign the 3.8 eV band at 300 K to the oxygen ad atom of the ad-ins×3 configuration. It follows that the observation of the 3.8 eV band can be associated either with a single-adsorption configuration (see above) or to a double-adsorption configuration. This statement is in agreement with calculations in Ref. 30 from which it was concluded that the electron photoemission band associated with an oxygen atom in ‘‘ad’’ position does not depend on the presence or not of oxygen atoms inserted into the Si backbonds.

Here we would like to discuss in more detail our assignment of the low-energy bands (3.8 and 5.1 eV) in the electron photoemission spectra, since it differs significantly from the recent results of Sakamoto *et al.*[21] We emphasize that the experimental conditions are different in both studies. Our data are recorded at a much lower temperature (30 K) than those of Sakamoto *et al.*,[21] which were recorded at 120 K. This has important consequences since the metastable ad-ins structure is not expected to exist at 120 K. Indeed from Lee and Kang’s calculations,[20] the ‘‘ad-ins’’ structure is predicted to disappear above 50 K. Furthermore, our observation of the metastable single adsorption configuration is based on measurements performed at $O_2$ coverages, where less than 10% of the silicon adatoms reacted, while measurements of Sakamoto *et al.*[21] were associated with $O_2$ coverages where more than 25% of the adatoms already reacted.

Sakamoto *et al.*[21] proposed assigning the two 3.8 and 5.1 eV bands to two electronic states ($\pi_g$ and $\pi_u$ respectively) of $O_2$ molecules adsorbed on top of a Si adatom and stabilized by coadsorbed oxygen atoms into the backbonds. In previous papers,[13] we assigned the 3.8 and 5.1 eV bands to two separate configurations made of $O_2$ molecules adsorbed on top of silicon adatoms. These two separate molecular configurations were given different geometries in order to explain the different temperature and photon incidence angle dependencies of the relative intensities of the two 3.8 and 5.1 eV bands.[13] From the more complete set of data presented in Sec. IV, we reach a somewhat different conclusion. To fully explain the temperature and $O_2$ exposure dependence of the 3.8 and 5.1 eV band intensities, it is no longer possible to assign them to specific adsorption configurations. The 3.8 and 5.1 eV bands are rather assigned to specific oxygen bonds, i.e., an oxygen atom in the ‘‘ad’’ position and an oxygen atom in the ins position, respectively. Within this model, the 3.8 and 5.1 eV bands are both associated with the same ‘‘ad-ins’’ configuration obtained at 30 K for $O_2$ exposures smaller than 0.02 L. At higher exposures the 3.8 eV band is associated with the oxygen ad atom of both single and double-adsorption configurations (‘‘ad-ins’’ and ‘‘ad-ins×3’’) while the 5.1 eV band is associated with oxygen ins atoms of mainly ad-ins configurations. At 300 K, the 3.8 eV band is associated with oxygen ad atoms of ‘‘ ad-ins×3’’ configurations, while the 5.1 eV band is associated with oxygen ins atoms mainly in the ‘‘ins-ins’’ configurations.

The exposure dependence of the 7 eV band intensity, which is associated with ins oxygen atoms,[23] is completely different from that of the 3.8 eV band. At 300 K, while the 3.8 eV band intensity, associated with ad atoms in ‘‘ad-ins×3’’ configurations, saturates with the disappearance of free adatom sites, the 7 eV band intensity still increases with exposure. This implies that at 300 K the 7 eV band is not only associated with ins atoms in the ‘‘ad-ins×3’’ configurations but also with ins atoms in ‘‘ins×3-tri’’ configurations (see Fig. 1). Conversely, at 30 K, the 7 eV band intensity is always lower than that of the 3.8 eV band, from which we conclude that the 7 eV band is mainly associated with ‘‘ad-ins×3’’ configurations.

A striking feature of all the experiments on the adsorption of $O_2$ on a Si(111) 7×7 surface is the time evolution of the adsorption configuration occupancies after $O_2$ exposure. This has been observed in electron photoemission,[4,9,12] ion desorption,[9] and scanning tunneling microscopy experiments[14,15] for both single- and double-adsorption configurations. These instabilities have very long characteristic lifetimes (of the order of several minutes) which vary with the experimental conditions. They have been ascribed to the metastability of the corresponding adsorption configurations. Although metastable adsorption configurations may well exist, a number of other processes can also account for the observed time evolutions. In a previous paper,[14] we demonstrated that traces of water molecules in the residual gas of the UHV chamber, even for residual gas pressures as low as $3\times10^{-11}$ mbar, can induce a reaction at oxygen adsorption configurations on a time scale similar to the lifetime of the observed metastable features. Here we have examined a phenomenon, which can explain the time evolution of $O_2$ adsorption configurations at low temperature (30 K). It consists of diffusion across the surface of weakly bound oxygen molecules, which react at single oxygen adsorption configurations and produce double-adsorption configurations.

## VI. CONCLUSION

The adsorption of $O_2$ on a Si(111) 7×7 surface is a complex process, and has given rise to a large number of studies with contradictory results. The reasons for this complexity and these contradictions are progressively understood. First, the $O_2$ adsorption configurations depend on both the temperature and the $O_2$ exposure. Our present results pointed out that the single-adsorption configurations are ‘ad-ins’ at 30 K and ‘ins-ins’ at 300 K. Second, the assignment of the electron photoemission bands is complex. Each band should be associated with a specific bond rather than with a specific adsorption configuration. In particular, our present results pointed out that the 3.8-eV band can be associated with a Si-O bond between a Si adatom and a single bonded O atom in the ad position of both the ad-ins and ad-ins×3 configurations. Consequently each band may be associated with several different oxygen adsorption configurations. Third, the time dependence of the adsorption configuration populations is a very puzzling problem. Here this phenomenon has been assigned to the diffusion across the surface of $O_2$ molecules able to react at single-adsorption configurations for producing double-adsorption configurations.

The association of ion photodesorption and electron photoemission experiments, on the one hand and recent theoretical calculations,[20,22,24] on the other hands has enabled us to obtain an insight into the adsorption of $O_2$ on a Si(111) 7×7 surface. At 30 K, $O_2$ molecules adsorb dissociatively on a Si adatoms giving rise to ‘ad-ins’ configurations, with an O atom in an ‘ad’ position and an O atom inserted into the Si backbond. At higher coverages, $O_2$ molecules dissociate on already reacted O ad-ins configurations giving rise to ‘ad-ins×3’ configurations. The ad-ins configuration is not observed at 300 K. It can be considered as a metastable precursor of the ‘ins-ins’ configuration, which is the single-adsorption configuration present at 300 K. At 30 K, the double-adsorption configurations are essentially ‘ad-ins×3’ whereas at 300 K they are both ‘ad-ins×3’ and ‘ad×3-tri.’

## APPENDIX A: EXPOSURE DEPENDENCE OF THE POPULATIONS OF ADSORPTION CONFIGURATIONS WITHIN THE MODEL OF REF. 14

Let us consider a clean silicon surface, with $N_t$ the total number of initial available silicon adsorption sites, exposed to $O_2$ molecules under a constant pressure $P$, so that the $O_2$ exposure $L$ at time $t$ is $L=P\times t$. An $O_2$ molecule may interact with an initial silicon adsorption site with a sticking coefficient $k_1$, producing single-adsorption configurations ($N_1$ configurations at exposure $L$), which decreases the available number of silicon adsorption sites ($N_i$ sites at exposure $L$). The $O_2$ molecule may also react on single-adsorption configurations with a sticking coefficient $k_2$, decreasing their number and producing double-adsorption configurations ($N_2$ configurations at exposure $L$). This adsorption kinetics was first suggested by scanning tunneling microscopy (STM) observations.[14] The kinetic equations describing the adsorption processes are the

$$\frac{dN_i}{dL}=-k_1N_i, \tag{A1}$$

$$\frac{dN_1}{dL}=k_1N_i-k_2N_1, \tag{A2}$$

$$\frac{dN_2}{dL}=k_2N_1. \tag{A3}$$

Using the initial conditions

$$N_i=N_t, \tag{A4}$$

$$N_1=0, \tag{A5}$$

$$N_2=0, \tag{A6}$$

the resolution of the system of differential equations provides the evolution with the exposure of the population of the initial adsorption site and the single- and double-adsorption configurations:

$$N_i=N_te^{-k_1L}, \tag{A7}$$

$$N_1=\frac{k_1N_t}{k_2-k_1}(e^{-k_1L}-e^{-k_2L}), \tag{A8}$$

$$N_2=\frac{N_t}{k_2-k_1}[k_2(1-e^{-k_1L})-k_1(1-e^{-k_2L})]. \tag{A9}$$

For low values of $L$,

$$N_i \approx N_t(1-k_1L), \tag{A10}$$

$$N_1 \approx k_1N_tL, \tag{A11}$$

$$N_2 \approx N_t\frac{k_1k_2}{2}L^2. \tag{A12}$$

It appears that, within the model of Ref. 14, in the low-exposure range, the population of single- (double-) adsorption configurations varies linearly (quadratically) with the exposure.

## APPENDIX B: FIT OF THE EXPOSURE DEPENDENCIES OF THE ION YIELD AND PHOTOEMISSION BAND INTENSITIES

Let us first consider the data recorded when the silicon sample is at 300 K. The exposure dependence of the $S_1$ band intensity can be fitted by a linear function for exposures lower than 0.4 L, and by an exponential function in the 0–2 L range (see Fig. 8). The value of $k_1$ (300 K) is deduced to be 1.1 $L^{-1}$. The exposure dependencies of the $O^+$ yield [see Fig. 3(a)] and of the 3.8 eV band [see Fig. 8(a)] can be exactly superimposed. They can be fitted by Eq. (A12) of Appendix A for exposures lower than 0.2 L (quadratic behavior) and by Eq. (A9) of Appendix A in the 0–2.4 L range (see Fig. 3). From these fits, we derive that the $O^+$ yield and the 3.8 eV band are associated with double-adsorption sites, and that the sticking coefficient $k_2$ (300 K) of $O_2$ on single-adsorption sites is 3 $L^{-1}$, higher than $k_1$ (300 K). This is in agreement with the STM observation that single-adsorption configurations are more reactive than the initial silicon adatom sites.[14]

Let us now consider the data recorded when the silicon sample is at 30 K. The exposure dependence of the $S_1$ band intensity can be fitted by a linear function for exposures lower than 0.1 L, and by an exponential one in the 0–0.45 L range (see Fig. 9). The value of $k_1$ (30 K) is deduced to be 5.5 $L^{-1}$, higher than $k_1$ (300 K) by a factor of 5. The sticking coefficient $k_1$ increases when lowering the temperature. The exposure dependencies of the $O^+$ yield and of the 3.8 eV band is linear in the 0–1-L range (see Fig. 3), which implies that they are associated with single-adsorption sites. Then the exposure dependencies become more complicated due to contributions from both single-and double-adsorption configurations with different photodesorption and photoemission cross sections.

---

*Email address: genevieve.comtet@ppm.u-psud.fr.
Present address: Laboratoire de Photophysique Moléculaire, Bât 210, Université de Paris-Sud, 91405 Orsay Cedex, France

[1] H. Ibach, H. D. Bruchmann, and H. Wagner, Appl. Phys. A: Solids Surf. **29**, 113 (1982).

[2] K. Edamoto, Y. Kubota, H. Kobayashi, M. Onchi, and M. Nishijima, J. Chem. Phys. **83**, 428 (1985).

[3] A. J. Schell-Sorokin and J. E. Dermuth, Surf. Sci. **157**, 273 (1985).

[4] U. Höfer, P. Morgen, W. Wurth, and E. Umbach, Phys. Rev. Lett. **55**, 2979 (1985); Phys. Rev. B **40**, 1130 (1989); P. Morgen, U. Höfer, W. Wurth, and E. Umbach, *ibid.* **39**, 3720 (1989).

[5] C. Silvestre and M. Shayegan, Phys. Rev. B **37**, 10 432 (1988); C. Silvestre, J. Hladky, and M. Shayegan, J. Vac. Sci. Technol. A **8**, 2743 (1990).

[6] P. Gupta, C. H. Mak, P. A. Coon, and S. M. George, Phys. Rev. B **40**, 7739 (1989).

[7] Ph. Avouris, In-Whan Lyo, F. Bozso, In-Whan Lyo, Ph. Avouris, B. Schubert, and R. Hoffmann, J. Phys. Chem. **94**, 4400 (1990).

[8] B. Schubert, P. Avouris, and R. Hoffmann, J. Chem. Phys. **98**, 7593 (1993); **98**, 7606 (1993).

[9] G. Dujardin, G. Comtet, L. Hellner, T. Hirayama, M. Rose, L. Philippe, and M. J. Besnard-Ramage, Phys. Rev. Lett. **73**, 1727 (1994).

[10] K. Sakamoto, K. Nakatsuji, H. Daimon, T. Yonezawa, and S. Suga, Surf. Sci. **306**, 93 (1994).

[11] P. Bratu, K. L. Kompa, and U. Höfer, Phys. Rev. B **49**, 14 070 (1994).

[12] B. Lamontagne, D. Roy, R. Sporken, and R. Caudano, Prog. Surf. Sci. **50**, 315 (1995).

[13] G. Comtet, G. Dujardin, L. Hellner, T. Hirayama, M. Rose, L. Philippe, and M. J. Besnard-Ramage, Surf. Sci. **331–333**, 370 (1995); G. Comtet, L. Hellner, G. Dujardin, and M. J. Besnard-Ramage, *ibid.* **352–354**, 7608 (1996).

[14] G. Dujardin, A. Mayne, G. Comtet, L. Hellner, M. Jamet, E. Le Goff, and P. Millet, Phys. Rev. Lett. **76**, 3782 (1996).

[15] R. Martel, Ph. Avouris, and I. W. Lyo, Science **72**, 385 (1996).

[16] G. Comtet, G. Dujardin, and L. Hellner, Europhys. Lett. **36**, 355 (1996).

[17] K. Sakamoto, S. Suto, and W. Uchida, Surf. Sci. **357**, 514 (1996).

[18] I. H. Hwang, R.-L. Lo, and T. T. Tsong, Phys. Rev. Lett. **78**, 4797 (1997); I. S. Hang, R. L. Lo, and T. T. Tsong, Surf. Sci. **399**, 173 (1998).

[19] K. Y. Kim, T. H. Shin, S. J. Han, and H. Kang, Phys. Rev. Lett. **82**, 1329 (1999).

[20] S. H. Lee and M. H. Kang, Phys. Rev. Lett. **82**, 968 (1999).

[21] K. Sakamoto, S. Doi, Y. Ushimi, and K. Ohtno, Phys. Rev. B **60**, R8464 (1999).

[22] T. Hoshino and Y. Nishioka, Phys. Rev. B **61**, 4705 (2000).

[23] S. H. Lee and M. H. Kang, Phys. Rev. B **61**, 8250 (2000).

[24] S. H. Lee and M. H. Kang, Phys. Rev. Lett. **84**, 1724 (2000).

[25] F. Matsui, H. W. Yeom, K. Amemiya, K. Tono, and T. Ohta, Phys. Rev. Lett. **85**, 630 (2000).

[26] G. R. Harp, Z. L. Han, and B. P. Tonner, J. Vac. Sci. Technol. A **8**, 2566 (1990).

[27] Dien Li, G. M. Bancroft, and M. Kasrai, Solid State Commun. **87**, 613 (1993).

[28] M. Azizan, R. Baptist, A. Brenac, G. Chauvet, and T. A. Nguyen Tan, J. Phys. (Paris) **48**, 81 (1987).

[29] J. E. Northrup, Phys. Rev. Lett. **57**, 154 (1986).

[30] Ph. Sonnet, L. Stauffer, and C. Minot, Surf. Rev. Lett. **6**, 1039 (1999).